Search for coherent structure within tokamak plasma turbulence

S. J. Zweben[a)]
California Institute of Technology, Pasadena, California 91125

(Received 27 August 1984; accepted 3 December 1984)

Two-dimensional tokamak edge density turbulence data are examined for possible coherent or organized structure. The spatial patterns of density fluctuations $\tilde{n}$ appear to consist of localized "blobs" of relatively high or low density which can move irregularly both radially and poloidally through the edge region. However, a statistical analysis of the lifetime, area, direction, speed, and amplitude of these blobs does not as yet suggest any organized structure associated with the blobs beyond that which can be described by time-averaged correlation functions.

I. INTRODUCTION

Recent developments in fluid turbulence have suggested that there may be underlying "coherent" or organized structure within flows which had previously been thought to be composed of unstructured, broadband turbulence.[1–4] In fluids these coherent structures often consist of large-scale vortices which can retain their geometry over many characteristic lengths of the motion[4] and which can significantly affect transport and mixing.[3]

It is possible that an understanding of the dynamics and interactions of such coherent structures may eventually lead to quasideterministic modeling of turbulent flows. However, these structures are often difficult to detect using single-point or even two-point correlation methods, since they can move irregularly through the fluid and are not necessarily periodic in time. Multipoint probe measurements or flow visualization techniques are then necessary in order to detect them.

Although plasmas are probably more complex than fluids such as air or water, somewhat similar organized plasma structures such as those associated with solitons, convective cells, or filamentation have been predicted theoretically[5–9] and previously observed in nontokamak plasmas.[10–12] Thus it seems worthwhile to investigate the detailed space-time structure of the turbulence in a tokamak plasma in order to search for such organized structure.

Previous measurements of tokamak density turbulence $\tilde{n}$ have been made using electromagnetic scattering and probes[13,14]; however, the data obtained so far have always been averaged over space and/or time (i.e., over many correlation volumes or autocorrelation times), so that a search for coherent structures analogous to those in fluid flows has not been attempted (and no such structure has yet been reported). This paper describes the first search for coherent or organized structure made using unaveraged local measurements of the 2-D (two-dimensional) density turbulence $\tilde{n}$. These measurements are made using a 2-D multiprobe array located in the edge–plasma region of the Caltech tokamak.

In Sec. II we describe the experimental setup, and in Section III are the experimental results. Section IV is the discussion, and in Sec. V is a summary.

II. EXPERIMENTAL SETUP

A. Caltech research tokamak

Most details concerning this tokamak have been described previously.[15,16] The plasma major radius is $R = 45$ cm, minor radius $a = 16$ cm, toroidal field on axis is $B_T = 3.5$ kG, plasma current $I = 20$ kA, line average density $n = 5\times10^{12}$ cm^{-3}, pulse length 10–15 msec, and typical energy confinement time = 0.5 msec.

For the experiments described here the tokamak was operated in the middle of its normal operation range without any localized limiters other than the support for the probe array itself (the edge plasma turbulence is relatively insensitive to the plasma conditions and to the presence of limiters over the normal range of operation of this machine[15]). All the data presented are taken during the steady-state (i.e., flat-current) phase of the discharge, for which the average density and temperature at $r/a = 0.8$ are typically $n = 10^{12}$ cm^{-3} and 25 eV.

B. The 2-D probe array

The results described below were obtained using the 2-D radial versus poloidal Langmuir probe array shown in Fig. 1. This array consists of a square matrix of $8\times8 = 64$ identical probes, each being 0.15 cm in diameter and length (in the toroidal direction) of 0.6 cm. The spacing between these probes of 0.26 cm is approximately the diameter of an ion gyro-orbit in this region of the plasma (evaluated at $T_i = T_e = 25$ eV), i.e., $r_s = \sqrt{T_e/M_i} = 0.15$ cm, so that the array is capable of resolving the smallest length scales of interest.

The total size of this array is 1.8 by 1.8 cm, which is about 1–2 correlation lengths of the $\tilde{n}$ turbulence.[16] This turns out to be an important limitation of this system, since the individual localized blobs of density can not be followed very far along the "flow." However, this array size represents a practical limit for square arrays, since the plasma begins to be perturbed for probe insertion distances above about 3 cm.

For all cases below, the probe array is at a fixed position in the edge plasma at the outer equatorial plane of the tokamak, where the probes themselves extended from 0.5 to 2.3 cm radially in past the outer wall. Note that probe support structure extends 0.6 cm radially in past the innermost row of probes and 1.5 cm poloidally past the upper and lower

a) Present address: Princeton Plasma Physics Lab, Princeton, New Jersey 08540.

 0031-9171/85/030974-09$01.90

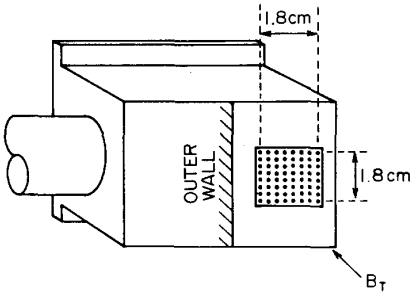

FIG. 1. Construction of the 2-D Langmuir probe array. There are 64 separate probes in an 8×8 radial versus poloidal (horizontal versus vertical) matrix which is inserted into the outer equatorial plane of the tokamak.

rows of probes. The poloidal extent of the 2-D array was made the same as the radial extent for the sake of simplicity. Note also that the probes point into the direction of the toroidal field and are mounted on the ion drift side of the probe support structure.

With this configuration these probes are clearly in the shadow of the probe support structure, which itself acts like a small limiter in this machine. Thus the results obtained for the 2-D structure refer, strickly speaking, only to the scrape-off layer plasma, i.e., the limiter shadow region. However, this probe design was motivated by previous single-probe observations that the $\tilde{n}$ turbulence levels and spectra within a limiter shadow region are very similar to those measured without any limiters.[15] This was checked in the present context by noting that the average poloidal correlation lengths, poloidal propagation speeds, relative fluctuation levels, and frequency spectra were all approximately the same when measured by this shadowed 2-D array and by an unshadowed 1-D probe array.[16] Furthermore, the 2-D results were independent of whether the probe support structure was grounded or floated (i.e., independent of the potential of the probe support structure with respect to the plasma). Because of these checks and also because of the similarity of the averaged $\tilde{n}(\omega,k)$ spectrum to that measured without any limiters by electromagnetic scattering experiments,[13,14] we can at least tentatively assume that the structure of edge density turbulence seen by this array is approximately the same as that which exists in the absence of the inserted array.

The probe tips for this array were gold-coated electrical pins that were mounted into a Macor insulating sheet. The local heat flux was low enough to avoid any damage to the probes or the insulator. The pins were sealed and supported from the inside of the probe support structure, which was itself made of stainless steel and generally grounded to the chamber wall.

The density fluctuations $\tilde{n}$ were measured as usual using the ion saturation currents J^+ drawn by the probe tips when they are biased typically -100 V dc. These ion saturation currents were measured using 64 separate bias circuits such as those described previously.[15] A specially built data recording system was constructed which was capable of digitizing all 64 channels, each at a rate of 1.6 MHz.[16] Thus the 2-D array data are taken over about 512×0.6 μsec $\cong 0.3$ msec for each discharge. This was long enough to sample several periods of the lowest frequencies of interest in this turbulence. The analog signal bandwidth of this system was 200 kHz. The relatively high digitization rate was used in order to produce a smoothly varying pattern in the film which was made from these same data.[17]

III. EXPERIMENTAL RESULTS

A. Average properties

The time- and space-averaged properties of the edge-plasma density turbulence are described elsewhere.[16] The relative fluctuation levels are $\tilde{n}/n = 0.2$–0.5, the frequency and wavenumber spectra are broad, and the autocorrelation times and correlation lengths are short, suggesting that the edge density is strongly turbulent.

The averaged poloidal and radial correlation lengths as determined from the cross-correlation functions are $L_p = 1.1$ cm and $L_r = 0.7$ cm, respectively, which are in the range predicted by edge–plasma turbulence models.[14] The poloidal propagation speeds (as determined from the delay times of the peaks of the cross-correlation functions) are typically in the ion diamagnetic drift direction, consistent with the large outward radial electric field in this region.[16] There was a slight trend for the average radial propagation speed to be inward rather than outward.

Aside from these average length scales and propagation speeds there was no evidence from the space-time averaged cross-correlation functions for any coherent structure within the edge density turbulence. In the following sections we examine the detailed, unaveraged 2-D space-time density patterns in order to search for possible organized structure that might underlie this apparently random plasma state.

B. 2-D space-time data

Two examples of the unaveraged 2-D space versus time patterns of $\tilde{n}$ are shown in Fig. 2. These patterns show the local relative $\tilde{n}$ across the 1.8×1.8 cm array over 10.8 μsec during the middle of two normal plasma discharges.

Each of the numbered frames in Fig. 2 contains 64 separate "pixels," one for each probe, which are arranged in an 8×8 matrix corresponding to the probe positions on the array (see Fig. 1). The pixels are each shaded with from 1 to 256 small dots according to the amplitude of $\tilde{n}$ at that place and time. The half-shading level (128) for each pixel is set to the average value of $\tilde{n}$ for that probe (for that discharge), and the darkest and lightest shadings are scaled to the highest and lowest values of $\tilde{n}$ for that probe, respectively. Thus each frame shows the pattern of *relative* density fluctuation across the array, the average values of $\tilde{n}$ having been subtracted out, and the amplitudes of $\tilde{n}$ being scaled for each probe separately. However, since the magnitude of $\tilde{n}$ is approximately constant across the array,[16] these patterns also represent (approximately) the actual distribution of the fluctuating component of $\tilde{n}$ across the array.

The raw data displays in Fig. 2 show at least one feature of the edge turbulence not evident from the averaged cross-correlation functions; namely, that the 2-D space-time structure of $\tilde{n}$ appears to consist of localized "blobs" which move through this radial-poloidal plane. In Fig. 2(a) a dark blob can be seen to enter the array from the upper left corner in

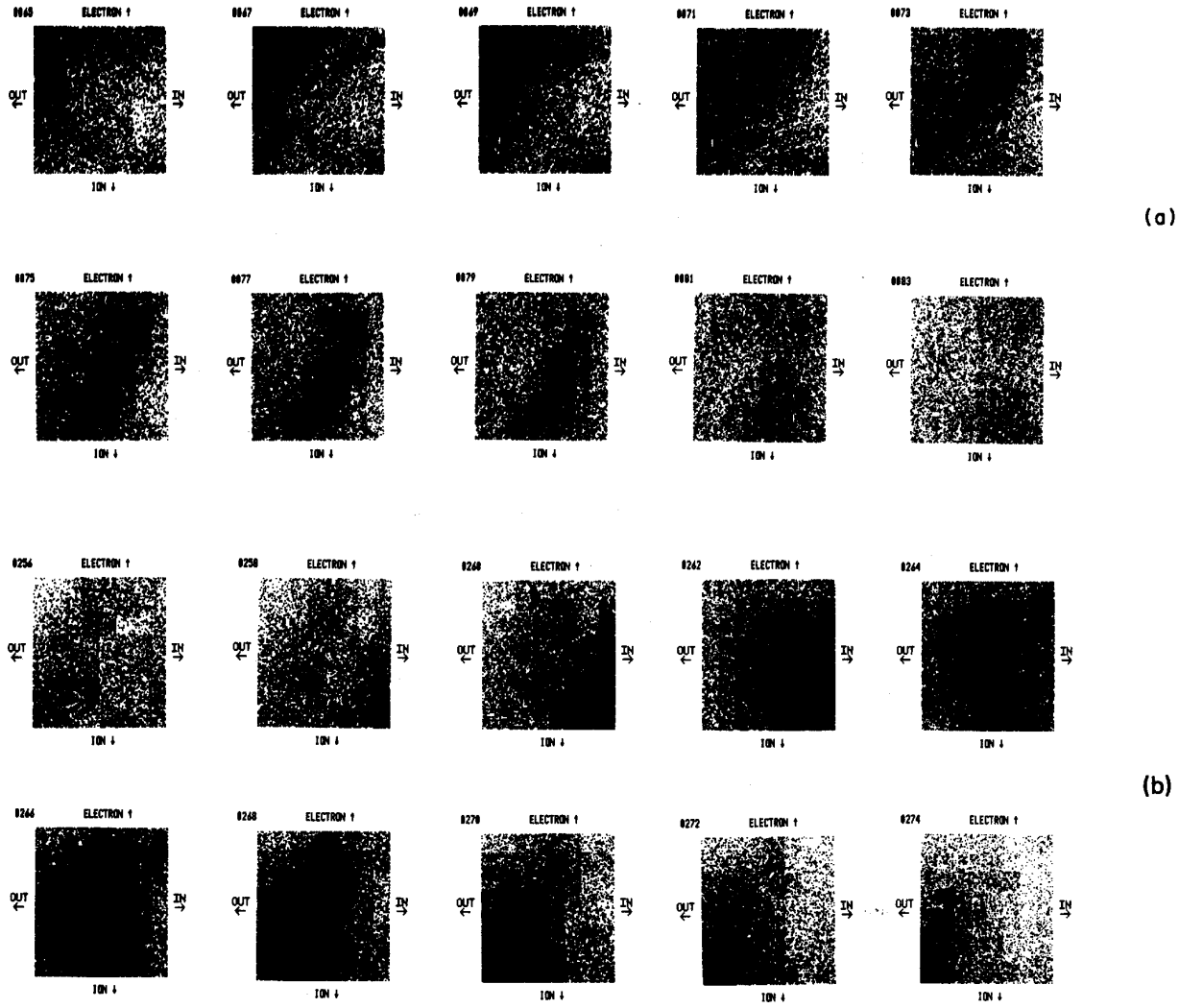

FIG. 2. Data on the 2-D space versus time patterns of edge density turbulence for two different shots (a) and (b). The localized dark regions are blobs of relatively higher plasma density which move through the edge region. The radially inward direction is toward the right, and the ion diamagnetic drift direction is down. The time between frames is 1.2 μsec.

the first frame, and to move toward the center and then gradually "dissipate" as it moves toward the lower right in successive frames (time between these frames is two sampling periods or 1.2 μsec). In Fig. 2(b) a blob appears to enter the array from the lower right and then move relatively unchanged toward the center and then toward the lower left in successive frames.

In the film which has been made from this and similar data,[17] a wide variety of blob sizes, shapes, and motions can be seen. In most cases the blobs appear to enter through the periphery of the array, and then to move across the array and out through another boundary. In a few cases a blob appears to grow spontaneously in the middle of the array or to dissipate before moving out of the array. Although there are both dark and light blobs (i.e., positive and negative local relative $\tilde{n}$ perturbations) we will concentrate only on the dark blobs in the discussion below.

Our present search for coherent structure will consist of an individual analysis of the sizes and motions of these blobs. The question is: do these blobs display any organized behavior or are they simply the "crests" of a random fluctuations field best described by the averaged $\tilde{n}(\omega,k)$ spectrum?

Of course, it is possible that there may be other more subtle types of coherent structure not describable in terms of blobs. However, the blob model seemed to be a natural first choice since it was clearly suggested by a qualitative (i.e., subjective) review of the data, and since it also seems to correspond to theoretically predicted coherent structures such as solitons (localized particle-like perturbations) or convective cells (plasma vorticies).

C. Identification of a blob

We have chosen to identify the existence and motion of a blob by the following constraints: (a) the center of the blob is defined as the "center of mass" of those pixels (i.e., normal-

ized $\tilde{n}$ signals) which lie above a certain intensity level, where by center of mass we mean the average position weighted by the intensity of each pixel, (b) in order to avoid the summing of two separate blobs, a minimum distance between the calculated center of mass and the location of the maximum pixel is also specified, and (c) in order to avoid possible discontinuities in the motion of center caused by unusually shaped blobs, a maximum distance between successive centers was also specified. The beginning time of a blob is defined as the time when a transition from 0 to 1 pixel above the preset intensity level occurs. The end time of a blob is defined by the time when the next transition to 0 pixels above the preset intensity level occurs, or when one of the conditions (b) or (c) above is violated.

The choice of these constraints was motivated by the desire for the existence and motion of the calculated blobs to match the impressions obtained from displays of the raw data such as shown in Fig. 2. The particular values used in the following analysis were: (a) the threshold intensity level was chosen to be 170 out of a possible maximum of 256, where a level of 128 represents the mean level of that pixel, (b) the minimum distance between the calculated center of mass and the maximum level was chosen to be 1.5 times the probe-to-probe separation, i.e., ~0.4 cm, and (c) the maximum jump between successive centers of mass was chosen to be three times the probe-to-probe separation, i.e., ~0.8 cm. Only those blob trajectories which lasted more than three successive time samples (i.e., 1.8 μsec) were retained. In general, under these constraints the calculated blob motions matched the perceived blob motions quite well (see below), although not all perceived blobs were counted [caused mainly by the constraint (a)]. The sensitivity of the calculated results to the values of the constraints was checked in part, as described below.

D. Blob trajectories

The trajectories of the centers of several typical blobs are shown in Fig. 3, including the two previously shown in the greyscale plots of Fig. 2. Each of these trajectories satisfied the constraints discussed in the previous section. Only one of these blobs is present in the array at any particular time.

Several properties of the blobs can be seen from this particular set of trajectories; for example, most blob centers move in the ion diamagnetic direction rather than in the electron diamagnetic direction, and most blobs either begin or end near the periphery of the array. On the other hand, it appears that there is no particular pattern or organized motion of the blob centers that would allow a prediction of its trajectory given, for example, its initial position or velocity.

A total set of 420 such blob trajectories was accumulated from 54 different tokamak discharges. These discharges were the same as used previously for the time-averaged analyses of the 2-D data.[16] For analysis of the correlation between two different blob properties (Sec. H), a subset of 77 trajectories from 12 discharges was used instead of the full set (this subset was randomly chosen, but contained only blobs which had a minimum lifetime of at least five timesteps instead of three timesteps as used for the full data set). The

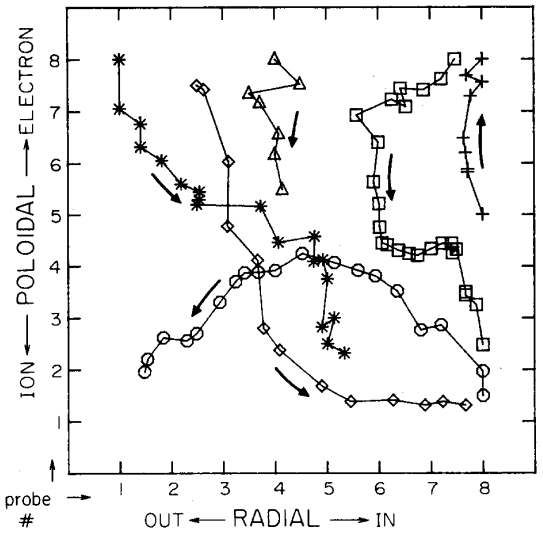

FIG. 3. Trajectories of several blob centers as they move across the 2-D array. The case shown in 2(a) and (b) are "*" and "O," respectively. Each point on these trajectories is separated by 0.6 μsec.

following sections contain a statistical analysis of these blobs aimed at discovering whether they display any organized structure.

E. Blob lifetime distribution

Of all the possible types of organized structure, perhaps the most basic would be that characterized by an unusually long lifetime of that particular structure in its own (moving) frame of reference. If this lifetime was much longer than a typical autocorrelation time (as measured at a fixed point), then one would suspect that the turbulence could be better described as a superposition of moving, independent objects rather than as a statistical distribution of Fourier components. Note that the broad frequency spectra measured experimentally a fixed point (or at a fixed k)[13,14] are not necessarily inconsistent with an unusually long blob lifetime, since the velocity and "impact parameter" of the blobs (with respect to a given point) can be variable.

In Fig. 4 is a histogram of the "lifetime" distribution of the blobs in the full data set, where by lifetime we mean the

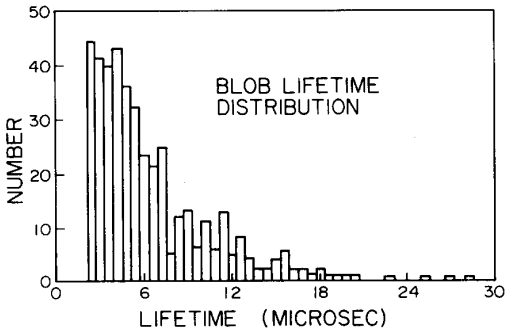

FIG. 4. Lifetime distribution of the full set of blobs detected in the array. The autocorrelation time at a fixed point is typically 6–8 μsec.

time over which a single blob can be followed across this array given the constraints discussed above. A convenient reference point is the autocorrelation time for the signal from a single probe, which is in the range $t_A = 6$–8 msec for this data.[16]

It should be noted at the outset that this distribution represents the measured "residence" time of the blobs within the boundary of this probe array and not the actual (total) lifetime of the blobs. A model for the influence of the finite probe size on the lifetime distribution is discussed in Sec. IV A.

The histogram of Fig. 4 shows that blob lifetimes of up to about three autocorrelation times ($\cong 21$ μsec) have been recorded in this sample. However, the fraction of detected blobs with a total lifetime of over 21 μsec is only about 1%, whereas the fraction of detected blobs with lifetimes below about two autocorrelation times (14 μsec) was over 90%. Note that the probability of detecting a blob at any particular time in the sample is about 17%, so that these blobs are a relatively common feature of the turbulence. A check was made of the sensitivity of this distribution to the threshold level chosen for identification of a blob, and approximately the same shape for the lifetime distribution was found for thresholds of 150 and 190 as for the 170 threshold shown here.

Apparently this broad distribution of blob lifetimes is more consistent with a random process having a timescale characteristic of the local autocorrelation time rather than with a well-defined or unusually long blob lifetime (e.g., soliton). However, it is important to note that most of the blobs either enter or leave the array through its periphery, thus producing an underestimate of the actual blob lifetime, as discussed in Sec. IV A.

F. Blob area distribution

Perhaps the next most significant kind of organized structure would be the existence of a particular size scale for the blobs. Note that a broad k spectrum as observed in the scattering and probe experiments[13,14] is not necessarily inconsistent with a relatively narrow range of blob sizes, since each blob would itself contain a sum of many spatial Fourier components.

In Fig. 5 is a histogram showing the area distribution of blob sizes for the full data set, where the area is defined as the largest number of pixels which are simultaneously above the intensity threshold during the lifetime of a blob. The maximum area of 64 pixels would correspond to a blob which at some time fills the array completely (recall that the average poloidal and radial correlation lengths were 1.1 cm and 0.7 cm, respectively, and that the array size was 1.8×1.8 cm). Obviously, the area so defined depends upon the threshold chosen; however, the shape of this area distribution was checked to be approximately the same for levels of 150 and 190 as for the level of 170 used here.

Again, this broad distribution seems to be more consistent with a random process related to the mean correlation lengths rather than with a fixed size scale for all blobs (a blob with the average correlation lengths would have an area of about 15 pixels). However, the same problem arises as with the lifetime distribution; namely, that some of the blobs never become entirely contained within this relatively small-sized array, and so the area of some blobs is underestimated (see Sec. IV A).

G. Blob net displacement

A third possible type of organized structure would involve the movement of the blob center; for example, blobs might preferably move at some particular angle or for some particular distance. Again, such "structure" would not generally be detected in the average cross-correlation functions.

In Fig. 6 is a scatter plot made using the full data set of the net radial versus net poloidal displacements of the blobs from their beginning to their end. The ratio of the number of blobs which move in the ion direction to those in the electron

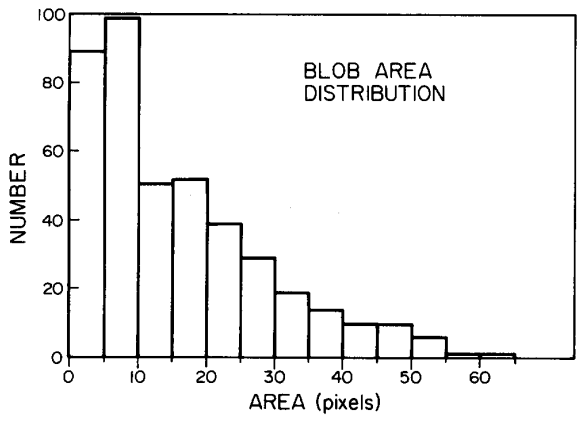

FIG. 5. Area distribution of the full set of blobs detected in the array. The area calculated from the average poloidal and radial correlation lengths is approximately 15 pixels.

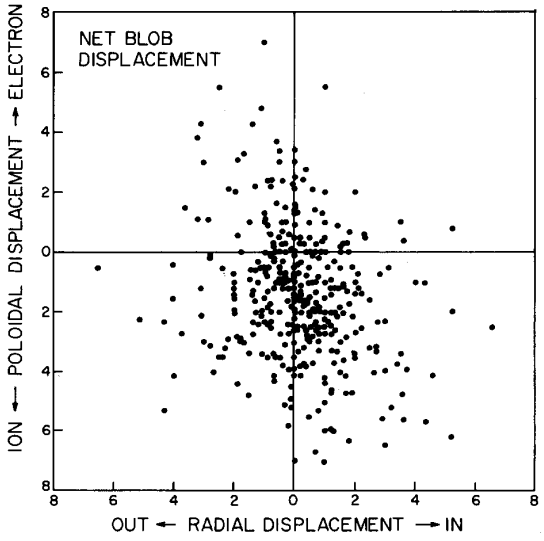

FIG. 6. Net radial versus net poloidal displacement of the blob center for the full data set. The trend for propagation in the ion diamagnetic drift direction is also seen in the time-averaged cross-correlation functions.

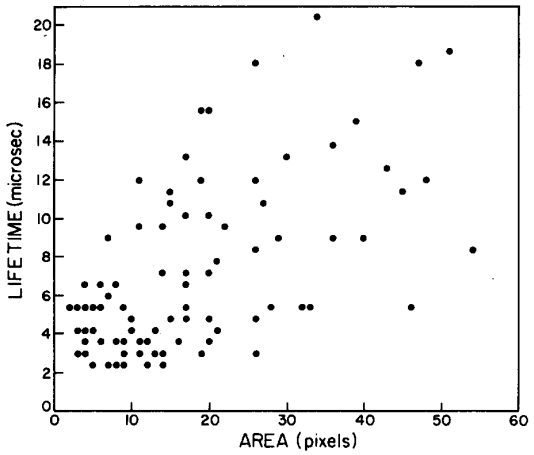

FIG. 7. Lifetime versus area for the subset of blob data. There is some correlation between long-lived and large-area blobs.

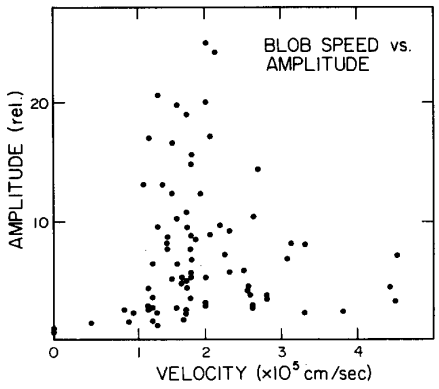

FIG. 9. Average speed versus amplitude for the subset of blob data. There is no clear correlation between these two blob properties. These speeds are similar to the propagation speeds derived from the cross-correlation functions.

direction is about 4:1, which is consistent with the predominant ion direction group velocities seen in the time-averaged cross-correlation functions.[16] The ratio of the number of blobs which move inward to those which move outward is only slightly above 1.0, which is also consistent with the slight tendency for an inward time-averaged group velocity.

However, there was apparently no preferred angle or distance of movement beyond that which could be described by the cross-correlation functions. Thus the blob movements are approximately as pictured in the trajectories in Fig. 3, i.e., they seem to move randomly across the array.

H. Correlations between two blob properties

Even though the lifetimes, areas, and movements of these blobs show no obvious organized structure, it is still possible that there are correlations between two different aspects of the same blob, for example, between blob lifetime and area. Such correlations might again be unobservable in the cross-correlation functions.

In Fig. 7 is a scatter plot of a blob lifetime versus area, where for this and for the next two plots the 77-blob subset was used instead of the full data set. From Fig. 7 it appears that there is some correlation between blob lifetime and area (i.e., lifetime increases with area); however, this is not too surprising since the blob identification process naturally follows larger blobs for a longer time (Sec. III C).

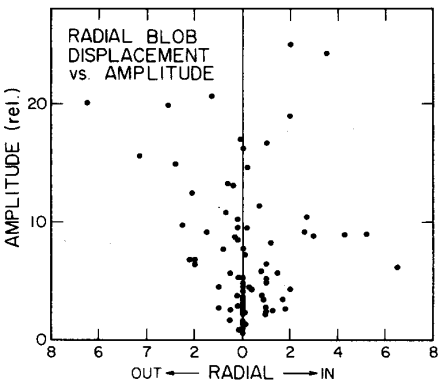

FIG. 8. Net radial displacement versus amplitude for the subset of blob data. There is no correlation between radial blob displacement and blob amplitude.

In Figs. 8 and 9 are two scatter plots showing the correlation of blob amplitude with net radial displacement and with average speed. The blob amplitude is defined as the average over the blob lifetime of the number of pixels above the intensity threshold times the average normalized intensity level of those pixels above the threshold. The blob speed is defined as the total distance moved by the blob center (summed after each time interval) divided by its total lifetime. These plots were motivated by the possibility that the blob radial displacement or speed could be dependent on the strength of its local perturbation.

The results on radial displacement in Fig. 8 show that there is no clear correlation between blob radial displacement and amplitude, as might be the case if the most intense blobs moved inward, for example. Similarly, the results on blob speed in Fig. 9 show that there is no clear correlation of blob speed with amplitude. Note that the tendency for more intense blobs to move farthest is generally the result of their longer average lifetime and not their higher speed (Fig. 7). The typical speed of $1\text{–}3\times10^5$ cm/sec is roughly consistent with (but somewhat less than) the poloidal propagation velocities measured by the time-averaged cross-correlation functions.

We conclude that no organized or coherent structure has yet been detected in this ensemble of blob data beyond that which had previously been determined from the time-averaged cross-correlation functions. Discussion of the limitations and possible extensions of this result are described below.

IV. DISCUSSION

A. Lifetime distribution

The lifetime distribution of Fig. 4 shows that a typical blob center can be followed for only about 10 μsec before it

leaves the array or violates one of the constraints discussed in Sec. III C. Since this lifetime t_B within the array is comparable to the autocorrelation time t_A measured at a fixed point, it appears that this distribution is more consistent with a set of random "crests" of an average $\tilde{n}(\omega)$ spectrum than with a soliton-like distribution with $t_B \gg t_A$, for example.

However, since most of the trajectories either enter or leave through the borders of the array, it is possible that the observed lifetime distribution significantly underestimates the actual lifetime of a blob. In the absence of data from a larger array, we can construct a simple blob model to try and fit the observed distribution with a hypothetical actual distribution.

The simplest model which preserves the 2-D nature of the blob motion is one in which the blobs all live for an actual time t_b, while moving at a constant velocity v_b in a straight line in a random direction in the radial-poloidal plane (the assumption of constant velocity is fairly well motivated by the results of Fig. 9; however, the actual trajectories are not straight lines and the directions are not quite random, as can be seen from Fig. 3). Thus the blob length l_b is such that $l_b = v_b t_b$ in this model.

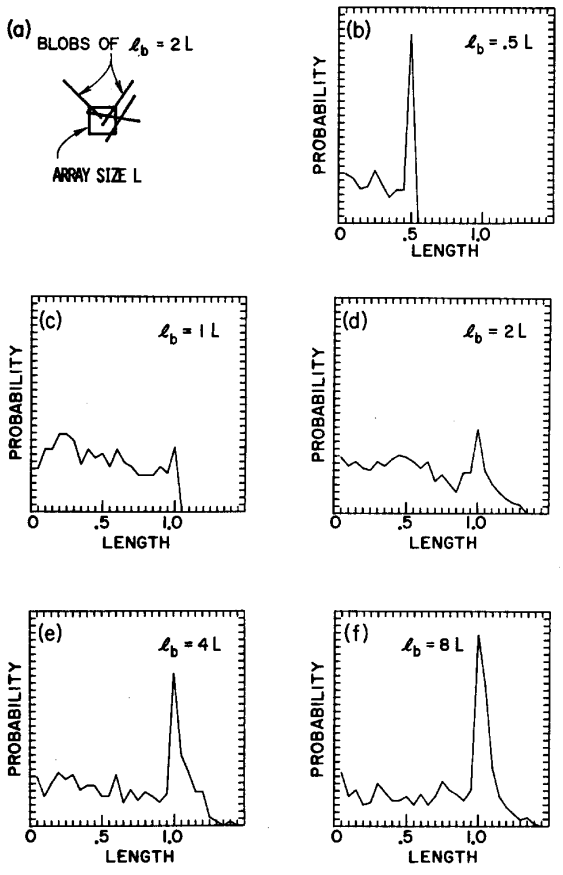

FIG. 10. Model resuls for the relative probability distribution versus overlapping length (normalized to the array side L) for various assumed blob lengths. In (a) is the geometry of the model, showing the array of side L and several randomly chosen blob trajectories of length $2L$ which partially overlap the array. In (b)–(f) are the overlapping-length (or time) distributions for various assumed blob lengths. A superposition of these distributions can be used to fit the observed lifetime distribution of Fig. 4.

If one defines the probe array as a square of side L in the radial-poloidal plane, as shown in Fig. 10(a), then one can start a blob at a random position and angle in this plane and then calculate the fraction of its length which overlaps the unit square (this length is proportional to the blob lifetime spent within the array). The distribution of overlapping lengths therefore simulates the experimental distribution of observed blob lifetimes t_B.

Some resulting model distributions are shown in Figs. 10(b)–10(f), where for each assumed blob length l_b a total of 500 overlapping trajectories were followed. For very short blob lengths $l_b \ll L$ most of the overlapping trajectories are fully within the square and the resulting overlapping length distribution is sharply peaked at l_b, i.e., the corresponding overlapping lifetime distribution would be peaked at $t_B = t_b$. However, for very long blob lengths $l_b \gg L$ (e.g., for soliton-like blobs) the resulting overlapping length distribution is sharply peaked near L, since few trajectories stop or start within the array and the most probable overlapping length is about L. For intermediate cases such that $l_b = (1\text{–}2)L$ the resulting distributions are rather broad, corresponding to a significant probability for the trajectory to only partially overlap the array.

Comparison of these model distributions with the observed lifetime distribution of Fig. 4 (assuming $l_b \sim t_b$) shows that none of these alone reproduces the experimental distribution. However, the closest fit comes from assuming a blob length of $l_b = (1\text{–}2)L$ [Figs. 10(d)–10(e)], i.e., a blob lifetime of $t_b = (1\text{–}2)L/v_b$. Given an approximate blob velocity of $v_b = 2\times 10^5$ cm/sec (Fig. 9), this implies an actual blob lifetime of $t_b = 10\text{–}20\,\mu$sec for the array size of $L = 1.8$ cm. This is roughly twice the autocorrelation time at a fixed point. Of course, a better fit to the experimental data can be made by building up a distribution function of lifetimes. However, this would probably not lead to realistic results given the many oversimplifications of this model (although it is clear that the observed distribution is also consistent with a small population of very long-lived blobs).

A rough check of this estimate for the actual blob lifetime (on average) can be made from an experimental measurement of the number of blobs which are observed to both start and end within the array (that is, more than one probe away from the array border). About 8% of the blobs (in the 77 blob subset) fall into this category. The model computation of the expected percentage to fall within this same subarea as a function of the assumed blob lifetime results in 8% for $t_b = 10\,\mu$sec, 26% for $t_b = 5\,\mu$sec, and 1% for $t_b = 15\,\mu$sec. Thus the best fit comes from an assumed actual lifetime of about $10\,\mu$sec.

Thus we can tentatively conclude that although most of the observed blobs do not spend their whole lifetimes within the array, it is likely that their actual lifetimes average only about 1–2 times the local (i.e., zero-dimensional) autocorrelation time. This can be qualitatively confirmed by noting that most blobs change their shape and/or size significantly during their passage across the array (see Fig. 2 in this paper and Fig. 8 of Ref. 16).

B. Relation to theory

Although the experimental results described in Sec. III did not show any clear evidence for the predominance of coherent structure in this edge density turbulence data, the analysis was inconclusive at several points: (a) coherent structure may be characteristic of only some fraction of the detected blobs (for instance, those with unusually long lifetimes), (b) the process of identification of a blob was somewhat arbitrary and oversimplified, (c) the array was too small to accurately identify or track the larger blobs (which might show more coherence than average) and (d) the blob motion in the parallel direction was not measured. Thus some further searches for structure within the turbulence are needed, and for these it would be useful to be guided by the theoretical possibilities.

Perhaps the most clear-cut example of a coherent structure theory of plasma turbulence applicable to the tokamak edge plasma is the solitary wave or modon solution to the 2-D drift wave turbulence equations, as calculated by Meiss and Horton.[6] These soliton-like solutions have the property that they can propagate in either the electron or the ion diamagnetic direction, which seems consistent with the experiment in that both directions can occur in the same region of plasma; also, the size and time scales of the modon distribution can reproduce a typical $\tilde{n}(\omega,k)$ spectrum. However, there are some features which are not yet consistent, for example the radial propagation is absent from this theory, and the theory predicts that positive perturbations should move in the electron direction while negative perturbations should move in the ion direction, which does not appear to be the case experimentally (although there is some uncertainty about the experimental correction for the dc radial electric field).

Numerical calculations of collisional drift wave turbulence applicable to the tokamak edge have been made by Wakatani and Hasegawa[8] and by Waltz.[19] These calculations reproduce quite well the observed 2-D spatial structure of the density turbulence (as shown in Fig. 2), and also show the presence of relatively long-lived isolated nonlinear vortex structures which can last significantly longer than a typical autocorrelation time. These computed structures may correspond to those blobs which last an unusually long time; however, no clearer correspondence with the experiment can be made at present. These models also predict fluctuation levels, spectra, and particle diffusion coefficients which are comparable to those measured in the edge plasma.[15,16]

The analytic nonlinear collisional drift wave theory of Terry and Diamond[20] includes the idea of "clumps" or density granulations as a component of the turbulence. These clumps have lifetimes which are comparable to several times the autocorrelation time and areas that are comparable to the mean correlation area, which appears to be roughly consistent with the blob distribution functions shown in Figs. 4 and 5. That is, this statistical turbulence theory involves structures which are less coherent than solitons but more coherent than expected from the average autocorrelation time of the turbulence. This theory also reproduces the experimental values for the average poloidal wavenumber, fluctuation level, and other properties of the edge turbulence.[15,16,21]

Other models involving some form of coherent structure are linear or nonlinear convective cells,[7,8,11] electrothermal filamentation,[9] and plasmon turbulence.[5] These models invoke instabilities mechanisms other than the usual density gradient driven drift wave.

Note that our search for organized structure did not concentrate on the relatively simple type of coherence associated with linear instabilities, since such a "global" space-time periodicity was not detected in either the frequency or the k spectra of this data.[16] Even when such periodicity is detectable in the averaged spectra, for example during the H mode in PDX,[22] this alone does not demonstrate the presence of coherent or organized structure in the sense that this term is used in fluid turbulence experiments. However, since there is yet no *a priori* definition of a coherent structure even for fluids,[2] the development of our definition of organized structure within plasma turbulence must follow further experimental and theoretical examples.

On the other hand, although we have suggested that these observed blobs seem to be more consistent with the "crests" of an averaged $\tilde{n}(\omega,k)$ spectrum rather than with a blob-like coherent structure, no quantitative comparisons with the space-time patterns generated by such spectra have yet been made. This should be rather straightforward, however, since the average frequency and k spectra are available from the experiment.[16]

C. Further experiments

As mentioned in Sec. I, the experience in ordinary fluid turbulence suggests that even when coherent or organized structure exists within a turbulent flow, it is often difficult to detect and to characterize quantitatively. This is in part because such structure can move irregularly through the fluid, making it difficult to track and measure.

A useful extention of the present results could be made by simply using a larger array (which can be done at least for the poloidal dimension), so that a more accurate lifetime distribution could be obtained. Much more analysis could also be done with the present data; for example, a possible rotation or swirling of some blobs is suggested from viewing the film, but has so far been difficult to quantify.

Another approach would be to analyze more carefully single-probe data in order to detect nonrandomness in the local $\tilde{n}(t)$; for example, non-Gaussian amplitude distribution functions or zero-crossing time distributions might indicate the presence of isolated coherent structure (experiments in fluid turbulence have used such single-point measurements to investigate "strange attractors" in the onset of turbulent flow[23]). Alternatively, an analysis of the higher-order correlation functions of two-probe data may allow calculation of the mode coupling coefficients, which could be at least as interesting as direct space-time identification of coherent structure.

It would also be very useful to develop an alternative to probe arrays for detecting the instantaneous 2-D structure of tokamak turbulence, since probes can be used only in the cool edge region of the plasma. Possible detection schemes

include 2-D imaging of the light spontaneously emitted by neutrals or ions,[24] fluorescence excitation of a 2-D layer of plasma with subsequent imaging,[3] holography, or shadowgraph photography. Particularly interesting would be a search for large-scale coherent structure ($k r_s \ll 1$), which if present could cause substantial plasma transport.[12] More information might also be extracted from multichannel scattering systems, for example, by cross-correlating different wavenumber signals originating from the same volume in order to search for some coherent structure.

V. SUMMARY

In this experiment we have used a compact array of Langmuir probes to obtain unaveraged, local 2-D space versus time data on density turbulence in the edge region of a tokamak plasma. These data were analyzed for the presence of possible coherent or organized structure. Specific conclusions include the following:

(1) The 2-D structure of the edge density turbulence consists of localized blobs of plasma which move irregularly both radially and poloidally through the edge region (Figs. 2 and 3).

(2) The lifetime distribution of these blobs is broad and roughly comparable to the local autocorrelation time t_A, although a small fraction of the detected blobs had lifetimes over $3t_A$ (Fig. 4).

(3) The area distribution of these blobs was also broad and roughly consistent with the area expected on the basis of the mean correlation lengths (Fig. 5).

(4) There was no clear coherent or organized structure or pattern detected for the ensemble blobs as a whole (Figs. 6–9).

It is important to note that no direct information about particle transport can be obtained from the blob trajectories alone, since these localized density perturbations can be caused by particle flow from any direction (analogously to water waves which can move without net fluid motion). Although similar blobs have been seen in the patterns of edge plasma potential,[16] a simultaneous density/potential measurement which could relate the blob trajectories to actual particle transport has not yet been made.

ACKNOWLEDGMENTS

I thank Roy Gould, Paulett C. Liewer, and Noel Corngold for helpful discussions and support during this work, J. Mahew for assistance in compiling the blob statistics, and T. Dupree and C. Ritz for discussions concerning coherent structures and mode-coupling analysis.

This research was supported by U. S. Department of Energy contract No. DE-FF03-84ER53173.

[1] *Role of Coherent Structures in Modelling Turbulence and Mixing, Lecture Notes in Physics*, edited by J. Jimenez (Springer-Verlag, Berlin, 1981), Vol. 136.
[2] A. K. M. F. Hussain, Phys. Fluids **26**, 2816 (1983).
[3] P. E. Dimotakis, R. C. Maike-Lye, and D. A. Papantoniou, Phys. Fluids **26**, 3193 (1982).
[4] B. Cantwell and D. Coles, J. Fluid Mech. **136**, 321 (1983).
[5] R. Z. Sagdeev, Rev. Mod. Phys. **51**, 1 (1979).
[6] J. D. Meiss and W. Horton, Phys. Fluids **25**, 1838 (1982).
[7] A. B. Hassam and R. M. Kulsrud, Phys. Fluids **22**, 2097 (1979).
[8] V. P. Pavlenko and J. Weiland, Nucl. Fusion **21**, 1283 (1981).
[9] M. G. Haines and F. Marsh, *Proceedings of the Ninth IAEA Conf. on Plasma Physics and Controlled Nuclear Fusion Research*, Baltimore, 1982 (IAEA, Vienna, 1982), Vol. II, p. 531.
[10] Y. Nakamura and I. Tsukabayashi, Phys. Rev. Lett. **52**, 2356 (1984).
[11] H. Pecseli, J. Juul Rasmussen, and K. Thomsen, Phys. Rev. Lett. **52**, 2148 (1984).
[12] A. Butcher Ehrhardt, H. A. Garner, G. A. Navratil, and R. S. Post, Phys. Fluids **24**, 1859 (1981).
[13] C. M. Surko and R. E. Slusher, Science **221**, 4613 (1983).
[14] P. C. Liewer, Nucl. Fusion (to be published).
[15] S. J. Zweben and R. W. Gould, Nucl. Fusion **23**, 1625 (1983).
[16] S. J. Zweben and R. W. Gould, Nucl. Fusion (to be published).
[17] A film of these edge turbulence patterns is available from the author.
[18] M. Wakatani and A. Hasegawa, Phys. Fluids **27**, 691 (1984).
[19] R. Waltz, submitted to Phys. Fluids.
[20] P. W. Terry and P. H. Diamond, University of Texas at Austin, Institute for Fusion Studies, Report No. 114, 1984.
[21] C. P. Ritz, R. D. Bengtson, E. J. Powers, and S. J. Levinson, submitted to Phys. Fluids.
[22] R. E. Slusher, C. M. Surko, J. F. Valley, T. Crowley, E. Mazzucato, and K. McGuire, Phys. Rev. Lett. **53**, 667 (1984).
[23] A. Brandstater, J. Swift, H. L. Swinney, A. Wolf, J. D. Farmer, E. Jen, and P. J. Crutchfield, Phys. Rev. Lett. **51**, 1442 (1983).
[24] S. J. Zweben, J. McChesney, and R. W. Gould, Nucl. Fusion **23**, 825 (1983).